



Published in final edited form as:

Nat Med. 2008 March ; 14(3): 331–336.

## Distinct roles of matrix metalloproteases in the early- and late-phase development of neuropathic pain

Yasuhiko Kawasaki<sup>1,4</sup>, Zhen-Zhong Xu<sup>1,4</sup>, Xiaoying Wang<sup>2,4</sup>, Jong-Yeon Park<sup>1</sup>, Zhi-Ye Zhuang<sup>1</sup>, Ping-Heng Tan<sup>1</sup>, Yong-Jing Gao<sup>1</sup>, Kristine Roy<sup>3</sup>, Gabriel Corfas<sup>3</sup>, Eng H. Lo<sup>2</sup>, and Ru-Rong Ji<sup>1</sup>

<sup>1</sup> Pain Research Center, Department of Anesthesiology, Brigham and Women's Hospital and Harvard Medical School, Boston, Massachusetts 02115

<sup>2</sup> Neuroprotection Research Laboratory, Departments of Neurology and Radiology, Massachusetts General Hospital and Harvard Medical School, Charlestown, Massachusetts 02129

<sup>3</sup> Division of Neuroscience, Children's Hospital and Harvard Medical School, Boston, Massachusetts 02115

### Abstract

Treatment of neuropathic pain, triggered by multiple insults to the nervous system, is a clinical challenge because the underlying mechanisms of neuropathic pain development remain poorly understood<sup>1-4</sup>. Most treatments do not differentiate between different phases of neuropathic pain pathophysiology and simply focus on blocking neurotransmission, producing transient pain relief. Here, we report that early and late phase neuropathic pain development after nerve injury require different matrix metalloproteinases (MMPs). After spinal nerve ligation, MMP-9 shows a rapid and transient upregulation in injured DRG primary sensory neurons consistent with an early phase of neuropathic pain, whereas MMP-2 shows a delayed response in DRG satellite cells and spinal astrocytes consistent with a late phase of neuropathic pain. Local inhibition of MMP-9 via an intrathecal route inhibits the early phase of neuropathic pain, whereas inhibition of MMP-2 suppresses late phase of neuropathic pain. Further, intrathecal administration of MMP-9 or MMP-2 is sufficient to produce neuropathic pain symptoms. Following nerve injury, MMP-9 induces neuropathic pain through interleukin-1 $\beta$  cleavage and microglia activation at early times, whereas MMP-2 maintains neuropathic pain through interleukin-1 $\beta$  cleavage and astrocyte activation at later times. Inhibition of MMP may provide a novel therapeutic approach for the treatment of neuropathic pain at different phases.

---

Matrix metalloproteinases (MMPs) are widely implicated in inflammation and tissue remodeling associated with various neurodegenerative diseases through the cleavage of the extracellular matrix proteins, cytokines, and chemokines<sup>5-10</sup>. We hypothesized that neuropathic pain and neuroinflammation may share similar mechanisms. Therefore, we set out to study the roles of the two major gelatinases MMP-2 and MMP-9, in the pathophysiology of neuropathic pain using a well-characterized animal model of L5 spinal nerve ligation (SNL)<sup>11</sup>.

Since nerve injury-induced changes in the dorsal root ganglion (DRG) are essential for the generation of neuropathic pain<sup>1</sup>, we examined gelatinase activity in injured (L5) DRGs.

---

Correspondence: Ru-Rong Ji, Department of Anesthesiology, Brigham and Women's Hospital, 75 Francis Street, Medical Research Building, Room 604, Boston, MA 02115 Tel: (617) 732-8852; Fax: (617) 730-2801; Email: rrji@zeus.bwh.harvard.edu.

<sup>4</sup>These authors contribute equally to this study.

#### COMPETING INTERESTS STATEMENT

The authors declare that they have no competing financial interests.

Gelatin zymography showed very low activity of MMP-9 in the naive DRG (Fig. 1a). SNL induced rapid but transient upregulation of MMP-9, peaking at 1 day and declining after 3 days. In contrast, MMP-2 showed delayed upregulation, occurring on day 7 and maintaining on day 21 (Fig. 1a). SNL also increased MMP-9 expression on day 1 but not day 10 (Fig. 1b). The active form of MMP-9 was weak and not well separated from pro-MMP-9 (Fig. 1a,b, supplementary Fig. 1a,b). MMP-9 was expressed in DRG neurons and more MMP-9+ neurons were found after SNL (Fig. 1c). In cultured DRG neurons, tumor necrosis factor-alpha (TNF- $\alpha$ ) and interleukin-1beta (IL-1 $\beta$ ), the proinflammatory cytokines that are rapidly produced after tissue injury, increased both the expression and release of MMP-9 (supplementary Fig. 1c,d). TNF- $\alpha$  inhibitor further suppressed SNL-induced MMP-9 upregulation (supplementary Fig. 1e). Interestingly, neuronal activity was sufficient to release MMP-9 from DRG neurons (supplementary Fig. 1f). In the spinal cord dorsal horn where secondary nociceptive neurons are localized, MMP-9 activity was very low, and SNL only moderately increased MMP-9 expression (supplementary Fig. 1g). MMP-9 in the spinal cord originated partly from dorsal root axonal transport from DRG neurons, because MMP-9 in the dorsal horn was colocalized with CGRP, a peptide that is expressed in nociceptive primary afferents (supplementary Fig. 1h).

Neuropathic pain is characterized by mechanical allodynia, i.e. painful responses to previously non-painful mechanical stimuli. To define the role of MMPs in neuropathic pain development, we used five different approaches: (1) small synthetic inhibitors, (2) endogenous peptide inhibitors, (3) small interfering RNAs, (4) exogenous MMP injection, and (5) knockout mice. To avoid systemic effects of drugs, we delivered them into spinal fluid via intrathecal (i.t.) administration, with the idea of targeting MMP in the DRG and spinal cord<sup>12</sup>.

First, we continuously infused a small synthetic anthranilic acid-based MMP-9 inhibitor<sup>13</sup> for one week via an osmotic pump. This treatment delayed the development of mechanical allodynia for 11 days (Fig. 2a). Continuous bolus injections of the inhibitor produced gradually decreasing anti-allodynic effect over time (supplementary Fig. 2a). Recombinant TIMP-1, an endogenous tissue inhibitor of MMP-9<sup>14</sup>, when given one day after SNL, was highly effective in attenuating allodynia. A single injection (4 pmol) reversed allodynia for more than 24 hours in the early phase (Fig. 2b). However, TIMP-1 had no effect on allodynia when given 10 days after nerve injury (supplementary Fig. 2b). In support of the results of MMP-9 inhibitors, small interfering RNA (siRNA, 2  $\times$  5  $\mu$ g, i.t.) targeted against MMP-9 *in vivo* successfully suppressed DRG MMP-9 activity and expression following SNL and delayed the development of allodynia (Fig. 2c, supplementary Fig. 3a-c). Conversely, A single injection of exogenous MMP-9 (1 pmol, i.t.) produced rapid mechanical allodynia, which recovered at 6 days (Fig. 2d).

To further confirm our pharmacological data, we assessed neuropathic pain in mice lacking MMP-9 (*Mmp9*<sup>-/-</sup>). SNL induced robust spontaneous pain in wild type FVB mice especially in the first 3 days, which was reduced in knockout mice (Fig. 2e). The early phase mechanical allodynia was also reduced in knockout mice (Fig. 2f). However, the neuropathic pain symptoms fully developed on day 10 in knockout mice (Fig. 2e, f). Taken together, our data strongly suggest a critical role of MMP-9 in the early development of neuropathic pain. Notably, our MMP-9 knockout mice are not inducible mutants so that compensatory adaptations (e.g., MMP-2 upregulation, see below) may have occurred during development. Apart from neuropathic pain, inflammatory pain was also reduced in MMP-9 deficient mice (supplementary Fig. 2c,d).

To define the mechanism by which MMP-9 induces neuropathic pain, we examined microglia activation in the spinal cord, an event essential for the pathogenesis of neuropathic pain<sup>15-18</sup>. MMP-9 injection evoked marked microglial activation, as indicated by increased expression of microglial marker OX-42 (Fig. 3a). Because we have previously shown that SNL

activates p38 MAP kinase in spinal microglia<sup>19</sup>, we asked whether this pathway can be triggered by exogenous MMP-9. After MMP-9 injection, phosphorylated-p38 (P-p38) was exclusively elevated in OX-42+ microglia (Fig. 3b). Further, spinal microglia and p38 activation after SNL was inhibited by MMP-9 siRNA treatment (Fig. 3a,b) and in MMP-9 deficient mice (supplementary Fig. 4). Importantly, allodynia after MMP-9 and SNL was reversed by a p38 inhibitor (Fig. 3c). Thus, p38 activation in spinal microglia may occur downstream of MMP-9 for mediating nerve injury-induced allodynia.

A critical substrate of MMP-9 could be IL-1 $\beta$ <sup>5,20</sup>, which is essential for chronic pain generation<sup>18,21,22</sup>. MMP-9 treatment increased the cleaved forms of IL-1 $\beta$  in the DRG (Fig. 3d). ELISA analysis, which mainly detects cleaved IL-1 $\beta$ , also showed IL-1 $\beta$  increase following MMP-9 treatment (Fig. 3e, supplementary discussion). Conversely, SNL-induced IL-1 $\beta$  cleavage was reduced in MMP-9 null mice (Fig. 3d) or after MMP-9 siRNA treatment (Fig. 3e). IL-1 $\beta$  was expressed in DRG neurons and some satellite cells. Further, IL-1 $\beta$  was colocalized with MMP-9 in DRG neurons (supplementary Fig. 5a). Importantly, inhibiting IL-1 $\beta$  signaling with a neutralizing antibody blocked allodynia triggered by both MMP-9 and SNL (Fig. 3f). Collectively, these data suggest that IL-1 $\beta$  may also occur downstream of MMP-9 for mediating nerve injury-evoked pain.

As a comparison, we also examined the role of caspase-1, a well-known IL-1 $\beta$  converting enzyme, in the SNL model. Unlike MMP-9, caspase-1 was expressed in DRG satellite cells and not upregulated after SNL (supplementary Fig. 5a,b). Intrathecal treatment of the caspase-1 inhibitor Ac-YVAD-CMK only moderately inhibited SNL-induced IL-1 $\beta$  cleavage in the DRG (supplementary Fig. 5c,d). In the spinal cord, IL-1 $\beta$  cleavage by SNL was also reduced in MMP-9 null mice and after MMP-9 siRNA treatment, and intrathecal MMP-9 increased IL-1 $\beta$  levels (supplementary Fig. 5e). In contrast, inhibition of spinal caspase-1, which showed no upregulation after SNL and which was expressed in some microglial cells, failed to inhibit IL-1 $\beta$  cleavage (supplementary Fig. 5f,g, supplementary discussion). Thus MMP-9 and caspase-1 may regulate IL-1 $\beta$  cleavage under different conditions.

As illustrated in schematic Fig. 3g, MMP-9 produces neuropathic pain symptoms via IL-1 $\beta$  cleavage and microglial p38 activation. MMP-9 and IL-1 $\beta$  may also be released from central terminals of DRG neurons. There are possible positive feedback loops between cytokines and MMP-9 in the DRG and between IL-1 $\beta$  and p38 in the spinal cord. Intrathecal IL-1 $\beta$  induces spinal p38 activation<sup>23</sup> and p38 activation further induces IL-1 $\beta$  release<sup>24</sup>. How does IL-1 $\beta$  increase pain sensitivity? In the DRG, IL-1 $\beta$  modulates the activity of sodium channels to increase the excitability of nociceptive neurons (supplementary discussion). In the spinal cord, IL-1 $\beta$  both enhanced excitatory synaptic transmission and reduced inhibitory synaptic transmission in spinal nociceptive neurons (data not shown).

As expected, SNL also caused a profound MMP-9 upregulation in the damaged spinal nerve (supplementary Fig. 6a), which will lead to demyelination by MMP-9 cleavage of myelin basal protein, a process that might be associated with neuropathic pain<sup>6,25</sup>. MMP-9 expression was low in dorsal root containing central axons but increased after SNL (supplementary Fig. 6a). Electromicroscopy study showed no sign of demyelination or degeneration in dorsal root axons either after SNL or intrathecal MMP-9 at an allodynia-producing dose (1 pmol, supplementary Fig. 6b-e). Neither did the MMP-9 injection cause apoptosis of dorsal horn neurons (supplementary Fig. 6f). Therefore, MMP-9-induced allodynia and microglia activation do not result from dorsal root degeneration.

Compared to MMP-9, MMP-2 upregulation after SNL demonstrated different spatial and temporal patterns: SNL induced a delayed upregulation of MMP-2 in the DRG and spinal cord (Figs. 1a, 4a, 4b). Unlike MMP-9, MMP-2 was found in satellite cells in the DRG (Fig. 4a).

In the spinal cord, MMP-2 was induced in GFAP+ astrocytes (Fig. 4b). Intrathecal administration of TIMP-2, an endogenous tissue inhibitor of MMP-2<sup>14</sup>, at a very low dose (4.5 pmol), reversed SNL-induced allodynia on day 10 (Fig. 4c). To determine whether neuropathic pain can be persistently attenuated by MMP-2 inhibition, we performed repeated injections of a small synthetic inhibitor of MMP-2 (N-arylsulfonyl-N-alkoxyaminoacetohydroxamic acid compound, see supplementary discussion). This treatment partly attenuated allodynia on day 1 but almost completely blocked allodynia in the following 10 days. Notably, the anti-allodynic effect lasted for additional 4 days after a final injection, suggesting an accumulating effect of the inhibitor (Fig. 4d). To exclude a role of MMP-9 in late phase neuropathic pain, we tested the MMP-2 inhibitor in MMP-9 null mice. Interestingly, this inhibitor produced more profound anti-allodynic effect in knockout mice, due to MMP-2 compensation in these mice (Fig. 4e, supplementary Fig. 7a). SNL-induced allodynia was also reversed by specific MMP-2 knockdown with a siRNA (Fig. 4f, supplementary Fig. 3d-g). Conversely, intrathecal infusion of MMP-2 produced allodynia (supplementary Fig. 7b).

How can MMP-2 maintain neuropathic pain? Since MMP-2 was also implicated in IL-1 $\beta$  cleavage<sup>5,20</sup>, we tested this possibility at late times after SNL. IL-1 $\beta$  cleavage in the DRG and spinal cord, at SNL day 10, was inhibited by MMP-2 siRNA (Fig. 4g). Consistently, intrathecal MMP-2 enhanced IL-1 $\beta$  cleavage (supplementary Fig. 7b). Allodynia was also reversed by neutralizing IL-1 $\beta$  in both wild type and MMP-9 null mice (supplementary Fig. 7c).

Recent studies proposed a role of spinal astrocytes in maintaining neuropathic pain<sup>12</sup>. In particular, ERK MAP kinase is activated in spinal astrocytes at late times of nerve injury (supplementary Fig. 7d), which is required for persistent allodynia in both rats<sup>26</sup> and mice (data not shown). Administration of MMP-2 siRNA or TIMP-2 reduced SNL-induced ERK activation in spinal astrocytes, indicating a role of MMP-2 in ERK activation (Fig. 4g, supplementary Fig. 7d). Further, in cultured astrocytes, IL-1 $\beta$  treatment activated ERK and released MMP-2 (supplementary Fig. 7e). As summarized in supplementary Fig. 7f, MMP-2 upregulation maintains neuropathic pain by IL-1 $\beta$  cleavage and astroglial activation of ERK. There is also a positive feedback from IL-1 $\beta$  to MMP-2, enhancing MMP-2 production.

In summary, our findings have revealed new mechanisms of neuropathic pain. First, we have demonstrated different temporal upregulation and cellular localization of MMP-9 and MMP-2. Second, we have shown that MMP-9 produced in the injured DRG neurons serves as one of the triggers for spinal microglia activation and neuropathic pain development and that MMP-9-induced pathophysiology involves IL-1 $\beta$  cleavage and microglia p38 activation. Third, we have illustrated that MMP-2 produces late phase neuropathic pain by IL-1 $\beta$  cleavage and astrocyte ERK activation. Finally, we have shown that endogenous inhibitors of MMP (TIMP-1 and TIMP-2) are powerful agents for suppressing neuropathic pain. Given unique role of MMP-9 and MMP-2 in early and late phase neuropathic pain, MMP-9 inhibition may alleviate some early phase neuropathic pain conditions induced by major surgeries (e.g. thoracotomy during cardiac surgeries) or chemotherapy<sup>3,4,27</sup>, whereas MMP-2 inhibition may attenuate established neuropathic pain conditions (e.g. diabetic neuropathy). Ideally, a dual inhibition of MMP-2/9 may alleviate neuropathic pain at different phases. However, the network responses of other MMPs and their roles in neuropathic pain remain to be assessed.

## METHODS

### Animals and surgery

Male adult Sprague-Dawley rats (200-260g) were purchased from Charles River Laboratories, and male MMP-9 null (*Mmp9*<sup>-/-</sup>) mice and FVB control wild type mice (25-35 g) were obtained from Jackson Laboratories. The knock-out mice are fertile and do not show difference

in overall weight and behavior compared with wild type mice. MMP-9 null mice were backcrossed to FVB background for more than 5 generations. All animal procedures performed in this study were approved by Harvard Medical School Animal Care Committee. The animals were anesthetized with sodium pentobarbital (50 mg/kg) or isoflurane. To produce a spinal nerve ligation, the L5 transverse process was removed to expose the L4 and L5 spinal nerves. The L5 spinal nerve was then isolated and tightly ligated with 6-0 silk thread. Sham surgery (exposure of the spinal nerves without ligation) was used as control. To produce inflammatory pain, carrageenan (2%, 20  $\mu$ l) was injected into a hindpaw of mice. See Supplementary methods for more details.

### Drugs and administration

We purchased MMP-9-inhibitor (Inhibitor-I), MMP-2 inhibitor (Inhibitor-III), and Ac-YVAD-CMK (caspase-1 inhibitor II) from Calbiochem, MMP-9, TIMP-1, and TIMP-2 from Chemicon, MMP-2, IL-1 $\beta$  and IL-1 $\beta$  neutralizing antibody from R & D, thalidomide (TNF $\alpha$  synthesis inhibitor) from Sigma. The drug doses were selected on the basis of previous reports and our preliminary studies. siRNAs targeting MMP-9 and MMP-2 and mismatch control siRNAs (21 bp) were synthesized by Dharmacon. To deliver siRNA into cells, polyethyleneimine, a cationic polymer, was used as a delivery vehicle to prevent degradation and enhance cell membrane penetration of siRNAs<sup>28</sup>. The drugs or their vehicles (DMSO, saline, or normal serum) were delivered intrathecally into cerebral spinal fluid via lumbar puncture or via osmotic pump through an intrathecally implanted catheter. See Supplementary methods for more details.

### Gelatin zymography

Animals were deeply anesthetized with isoflurane and transcardially perfused with PBS. DRGs, spinal nerves, dorsal roots, and spinal dorsal horn segments (L5) were rapidly dissected and homogenized in SDS sample buffer containing proteinase inhibitors. Ten micrograms of proteins were loaded per lane into the wells of precast gels (10% polyacrylamide minigels containing 0.1% gelatin, Novex). After electrophoresis, each gel was incubated with 100 ml of development buffer<sup>8</sup>. Commercial MMP-9 and MMP-2 were used as standards. See Supplementary methods for more details.

### Western blotting

Animals were transcardially perfused with PBS, and the DRGs, spinal nerves, dorsal roots, and spinal cord segments were rapidly removed and homogenized in a lysis buffer containing a cocktail of proteinase inhibitors and phosphatase inhibitors. The protein concentrations were determined by BCA Protein Assay (Pierce), and 30  $\mu$ g of proteins were loaded and separated on SDS-PAGE gel (4-15%, Bio-Rad). After the transfer, the blots were incubated overnight at 4°C with polyclonal antibody against MMP-9 (1:1000, Chemicon), MMP-2 (1:1000, Torrey Pines), IL-1 $\beta$  (1:1000, Chemicon), caspase-1 (1:500, Abcam) and pERK (1:1000, Cell Signaling). For loading control, the blots were probed with  $\beta$ -tubulin or ERK2 antibody.

### Immunohistochemistry

Animals were terminally anesthetized with isoflurane and perfused through the ascending aorta with saline followed by 4% paraformaldehyde. DRG and spinal cord tissues were excised and postfixed in the same fixative overnight. Tissue sections were cut in a cryostat and processed for immunofluorescence. All the sections were blocked with 2% goat serum, and incubated over night at 4°C with primary antibody, followed by Cy3- or FITC- conjugated secondary antibody. For double immunofluorescence, sections were incubated with a mixture of polyclonal and monoclonal primary antibodies followed by a mixture of FITC- and CY3- conjugated secondary antibodies. The specificity of immunostaining and antibodies was tested



by (1) omission of the primary antibody and (2) absorption of antibodies with respective peptide antigens. See more details in Supplementary methods.

### **Electromicroscopy examination**

The L5 dorsal roots close to the L5 DRGs were collected and fixed in 4% paraformaldehyde and 2.5% glutaraldehyde for 48 h at 4°C, then washed in PBS, osmicated, dehydrated, and embedded in epoxy. Ultrathin sections were cut, collected on cellodin-coated single-slot grids, stained with uranyl acetate and lead citrate, and photographed with a Jeol 1200EX electron microscope<sup>29</sup>.

### **ELISA**

Rat IL-1 $\beta$  ELISA kit was purchased from R & D Systems. IL-1 $\beta$  ELISA was performed according to manufacturer's protocol using 100  $\mu$ g proteins. The standard curve was included in each experiment.

### **Primary DRG culture**

DRGs were aseptically removed from 2-3 weeks rats and digested with collagenase (1.25 mg/ml)/dispase-II (2.4 units/ml) for 90 min, followed 0.25% trypsin for 8 min at 37°C. Cells were plated onto poly-D-lysine/laminin-coated slide chambers or poly-D-lysine-coated plates and grown in a neurobasal defined medium (Gibco). The DRG neurons were grown for 24 hours before experiments. See Supplementary methods for more details.

### **Primary astrocyte culture**

Astroglial cultures were prepared from cerebral cortexes of neonatal rats. The meninges were removed from cortexes in Hank's buffer. Cells were plated at  $2.5 \times 10^5$  /ml in a medium containing 15% FBS in low glucose DMEM and maintained for 3 weeks. The medium was replaced twice a week first with 15% FBS, then with 10% FBS, finally with 10% horse serum.

### **Behavioral analysis**

Animals were habituated to the testing environment daily for at least two days before baseline testing. For testing mechanical sensitivity, animals were kept in boxes on an elevated metal mesh floor and allowed 30 min for habituation before examination. The plantar surface of each hind paw was stimulated with a series of von Frey hairs with logarithmically incrementing stiffness (Stoelting), presented perpendicular to the plantar surface. The 50% paw withdrawal threshold was determined using Dixon's up-down method. To measure spontaneous pain in mice, we counted the numbers of paw flinches over a 2-minute period and averaged the numbers after 3 trials.

### **Quantification and statistics**

The density of specific MMP bands from gelatin zymography and Western blotting and the density of immunoreactive DRG neurons were measured with a computer-assisted imaging analysis system. The number of immunoreactive cells in the medial superficial laminae (I-III) of spinal cord was counted (see more details in Supplementary methods). Data were expressed as Mean  $\pm$  SEM. Differences between groups were compared using student t-test or ANOVA. The criterion for statistical significance was  $p < 0.05$ .

### **Supplementary Material**

Refer to Web version on PubMed Central for supplementary material.

## ACKNOWLEDGMENT

The work was supported in part by NIH R01-DE17794, R01-NS54362, and TW7180 to RRJ, and R01-NS37074, R01-NS48422, R01-NS56458, P01-NS55104, and P50-NS10828 to EHL.

## References

1. Ji RR, Strichartz G. Cell signaling and the genesis of neuropathic pain. *Sci.STKE* 2004;2004:reE14. [PubMed: 15454629]
2. Tsuda M, Inoue K, Salter MW. Neuropathic pain and spinal microglia: a big problem from molecules in “small” glia. *Trends Neurosci* 2005;28:101–107. [PubMed: 15667933]
3. Woolf CJ, Mannion RJ. Neuropathic pain: aetiology, symptoms, mechanisms, and management. *Lancet* 1999;353:1959–1964. [PubMed: 10371588]
4. Kehlet H, Jensen TS, Woolf CJ. Persistent postsurgical pain: risk factors and prevention. *Lancet* 2006;367:1618–1625. [PubMed: 16698416]
5. Parks WC, Wilson CL, Lopez-Boado YS. Matrix metalloproteinases as modulators of inflammation and innate immunity. *Nat.Rev.Immunol* 2004;4:617–629. [PubMed: 15286728]
6. Chattopadhyay S, Myers RR, Janes J, Shubayev V. Cytokine regulation of MMP-9 in peripheral glia: Implications for pathological processes and pain in injured nerve. *Brain Behav Immun* 2007;21:561–568. [PubMed: 17189680]
7. Rosenberg GA. Matrix metalloproteinases in neuroinflammation. *Glia* 2002;39:279–291. [PubMed: 12203394]
8. Wang X, et al. Effects of matrix metalloproteinase-9 gene knock-out on morphological and motor outcomes after traumatic brain injury. *J.Neurosci* 2000;20:7037–7042. [PubMed: 10995849]
9. Yong VW. Metalloproteinases: mediators of pathology and regeneration in the CNS. *Nat.Rev.Neurosci* 2005;6:931–944. [PubMed: 16288297]
10. Zhao BQ, et al. Role of matrix metalloproteinases in delayed cortical responses after stroke. *Nat.Med* 2006;12:441–445. [PubMed: 16565723]
11. Kim SH, Chung JM. An experimental model for peripheral neuropathy produced by segmental spinal nerve ligation in the rat. *Pain* 1992;50:355–363. [PubMed: 1333581]
12. Zhuang ZY, et al. A peptide c-Jun N-terminal kinase (JNK) inhibitor blocks mechanical allodynia after spinal nerve ligation: respective roles of JNK activation in primary sensory neurons and spinal astrocytes for neuropathic pain development and maintenance. *J.Neurosci* 2006;26:3551–3560. [PubMed: 16571763]
13. Levin JI, et al. The discovery of anthranilic acid-based MMP inhibitors. Part 3: incorporation of basic amines. *Bioorg.Med.Chem.Lett* 2001;11:2975–2978. [PubMed: 11677139]
14. Murphy G, Willenbrock F. Tissue inhibitors of matrix metalloendopeptidases. *Methods Enzymol* 1995;248:496–510. [PubMed: 7674941]
15. Coull JA, et al. BDNF from microglia causes the shift in neuronal anion gradient underlying neuropathic pain. *Nature* 2005;438:1017–1021. [PubMed: 16355225]
16. Raghavendra V, Tanga F, DeLeo JA. Inhibition of microglial activation attenuates the development but not existing hypersensitivity in a rat model of neuropathy. *J.Pharmacol.Exp.Ther* 2003;306:624–630. [PubMed: 12734393]
17. Tsuda M, et al. P2X4 receptors induced in spinal microglia gate tactile allodynia after nerve injury. *Nature* 2003;424:778–783. [PubMed: 12917686]
18. Watkins LR, Milligan ED, Maier SF. Glial activation: a driving force for pathological pain. *Trends Neurosci* 2001;24:450–455. [PubMed: 11476884]
19. Jin SX, Zhuang ZY, Woolf CJ, Ji RR. p38 mitogen-activated protein kinase is activated after a spinal nerve ligation in spinal cord microglia and dorsal root ganglion neurons and contributes to the generation of neuropathic pain. *J.Neurosci* 2003;23:4017–4022. [PubMed: 12764087]
20. Schonbeck U, Mach F, Libby P. Generation of biologically active IL-1 beta by matrix metalloproteinases: a novel caspase-1-independent pathway of IL-1 beta processing. *J.Immunol* 1998;161:3340–3346. [PubMed: 9759850]

21. Samad TA, et al. Interleukin-1beta-mediated induction of Cox-2 in the CNS contributes to inflammatory pain hypersensitivity. *Nature* 2001;410:471–475. [PubMed: 11260714]
22. Sweitzer S, Martin D, DeLeo JA. Intrathecal interleukin-1 receptor antagonist in combination with soluble tumor necrosis factor receptor exhibits an anti-allodynic action in a rat model of neuropathic pain. *Neuroscience* 2001;103:529–539. [PubMed: 11246166]
23. Sung CS, et al. Inhibition of p38 mitogen-activated protein kinase attenuates interleukin-1beta-induced thermal hyperalgesia and inducible nitric oxide synthase expression in the spinal cord. *J.Neurochem* 2005;94:742–752. [PubMed: 16033422]
24. Clark AK, et al. Rapid co-release of interleukin 1beta and caspase 1 in spinal cord inflammation. *J.Neurochem* 2006;99:868–880. [PubMed: 16942597]
25. Inoue M, et al. Initiation of neuropathic pain requires lysophosphatidic acid receptor signaling. *Nat.Med* 2004;10:712–718. [PubMed: 15195086]
26. Zhuang ZY, Gerner P, Woolf CJ, Ji RR. ERK is sequentially activated in neurons, microglia, and astrocytes by spinal nerve ligation and contributes to mechanical allodynia in this neuropathic pain model. *Pain* 2005;114:149–159. [PubMed: 15733640]
27. Dworkin RH, et al. Advances in neuropathic pain: diagnosis, mechanisms, and treatment recommendations. *Arch.Neurol* 2003;60:1524–1534. [PubMed: 14623723]
28. Tan PH, Yang LC, Shih HC, Lan KC, Cheng JT. Gene knockdown with intrathecal siRNA of NMDA receptor NR2B subunit reduces formalin-induced nociception in the rat. *Gene Ther* 2005;12:59–66. [PubMed: 15470478]
29. Chen S, et al. Disruption of ErbB receptor signaling in adult non-myelinating Schwann cells causes progressive sensory loss. *Nat.Neurosci* 2003;6:1186–1193. [PubMed: 14555954]



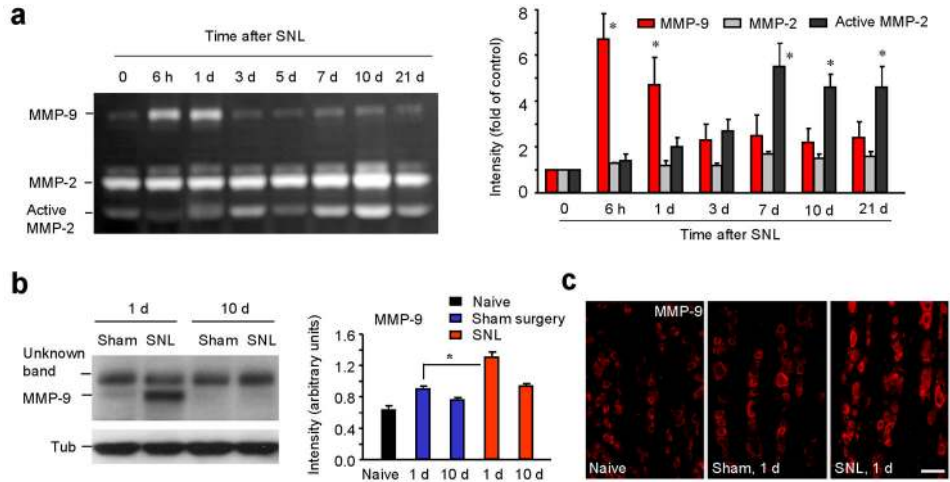


**Figure 1. Upregulation of MMP-9 in the DRG after spinal nerve ligation (SNL)**

(a) Gelatin zymography shows a time course of MMP-9 and MMP-2 activity in the injured L5 DRG of SNL rats. Right panel shows intensity of specific MMP bands, expressed as fold change over non-injured control. \*  $p < 0.05$ , compared to control ( $n = 5$ ). (b) MMP-9 Western blotting in the L5 DRG of sham and SNL rats. Right panel, quantification of MMP-9 band intensity (\*  $p < 0.05$ ,  $n = 3$ ). (c) MMP-9 immunohistochemistry in the L5 DRG of control and SNL rats. Note that MMP-9 is expressed in DRG neurons. Scale, 50  $\mu\text{m}$ .

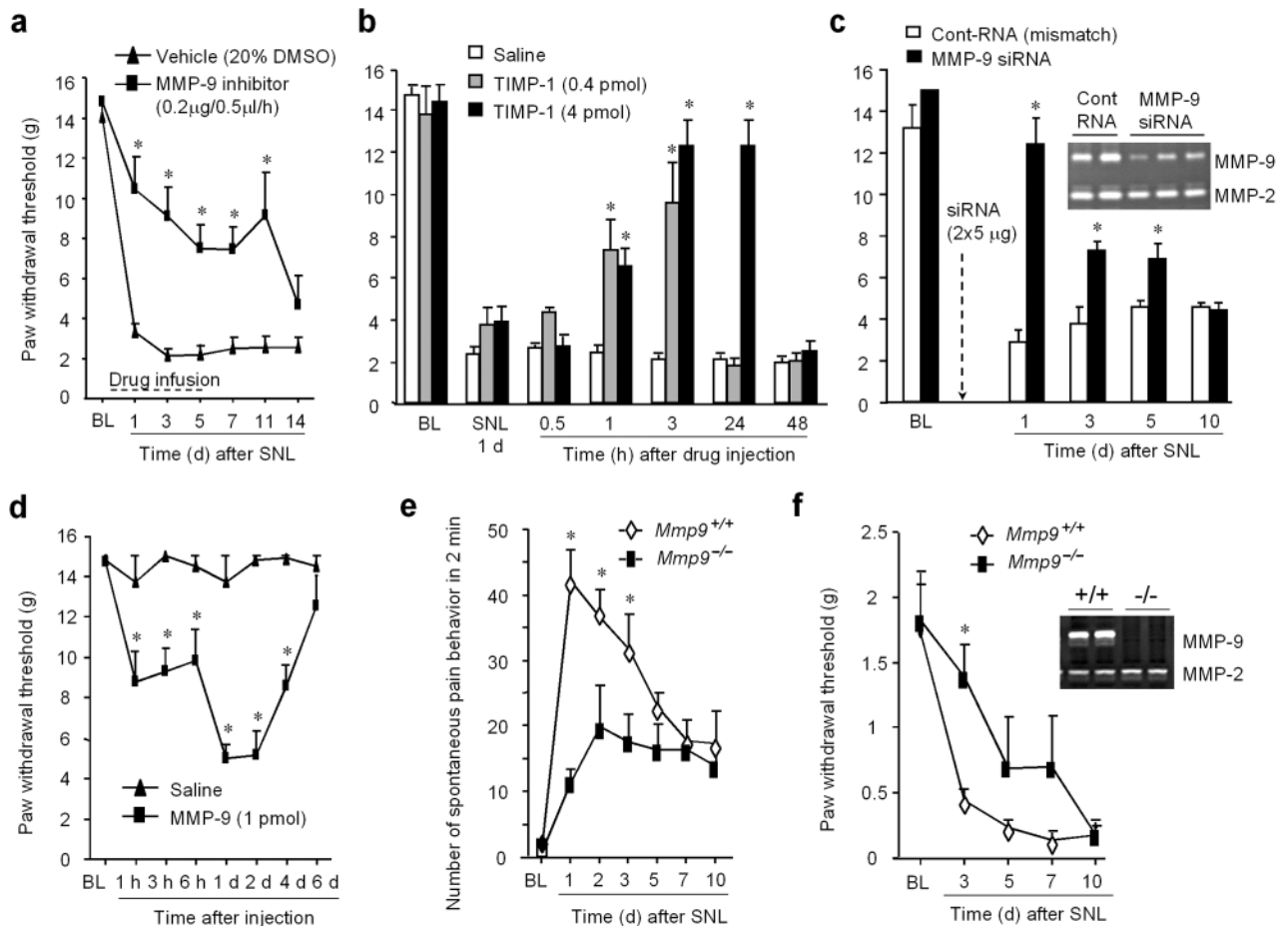


### Figure 2. MMP-9 is both required and sufficient for producing neuropathic pain symptom

(a) Persistent infusion of MMP-9 inhibitor delays the development of mechanical allodynia in SNL rats. The inhibitor or vehicle (20% DMSO) was intrathecally infused via an osmotic pump (0.5 μl/h, 7 days) starting 2 days before SNL (\*  $p < 0.05$ , compared to corresponding vehicle control,  $n = 6$ ). BL indicates baseline. (b) Reversal of mechanical allodynia by endogenous MMP-9 inhibitor TIMP-1 in SNL rats (\*  $p < 0.05$ , compared to saline,  $n = 6$ ). (c) Pretreatment of MMP-9 siRNA (2 × 5 μg, i.t.) delays the development of mechanical allodynia in SNL rats (\*  $p < 0.05$ , compared to respective mismatch control RNA,  $n = 9$ ). Insert, gelatin zymography showing knockdown of MMP-9 but not MMP-2 by MMP-9 siRNA in the DRG on SNL day 1. (d) Intrathecal administration of MMP-9 induces rapid but reversible mechanical allodynia in rats (\*  $p < 0.05$ , compared to saline control,  $n = 12$ ). (e) MMP-9 null mice show a reduction in SNL-induced spontaneous pain at early times (\*  $p < 0.05$ , compared to wild type mice,  $n = 6$ ). Spontaneous pain was evaluated by counting the number of flinches of affected hindpaws over a 2-minute period. (f) MMP-9 null mice show a reduction of mechanical allodynia at early times after SNL (\*  $p < 0.05$ , compared to wild type mice,  $n = 6$ ). Insert, gelatin zymography showing absence of MMP-9 in MMP-9 null mice.

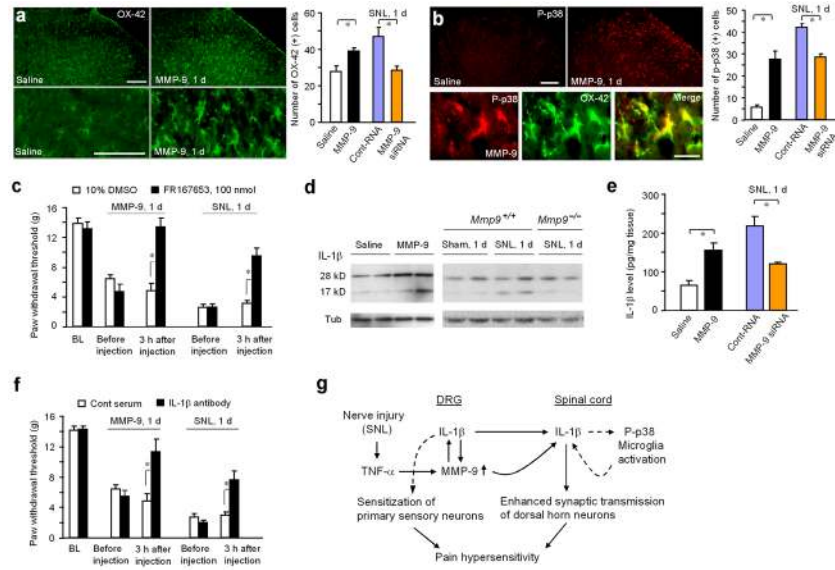


**Figure 3. MMP-9 produces neuropathic pain via microglia activation and IL-1 $\beta$  signaling**  
**(a)** Immunostaining of microglia surface marker OX-42 (CD11b) in rat dorsal horn after intrathecal saline or MMP-9 (1 pmol). Lower panel, high magnification of microglia. Scales, 50  $\mu$ m. Right panel, number of OX-42+ microglia following treatment of MMP-9 and MMP-9 siRNA ( $2 \times 5 \mu$ g) in rats ( $* p < 0.05, n = 4$ ). **(b)** Immunostaining of phospho-p38 (P-p38) in the dorsal horn after intrathecal MMP-9 (1 pmol). Low panel, colocalization of P-p38 and OX-42 in spinal microglia after MMP-9 treatment. Scales, 50 (upper) and 10  $\mu$ m (lower). Right panel, number of P-p38+ cells in the dorsal horn following treatment of MMP-9 and MMP-9 siRNA ( $* p < 0.01, n = 4$ ). **(c)** p38 inhibitor FR167653 (100 nmol, i.t.) blocks mechanical allodynia induced either by MMP-9 (1 pmol) or SNL ( $* p < 0.05, n = 6$ ). **(d)** Left panel: intrathecal MMP-9 (1 pmol) induces IL-1 $\beta$  cleavage in the DRG. Right panel, IL-1 $\beta$  cleavage after SNL is reduced in MMP-9 null mice. **(e)** ELISA shows DRG IL-1 $\beta$  levels after treatment of MMP-9, SNL, and MMP-9 siRNA ( $*, p < 0.05, n = 4-6$ ). **(f)** Mechanical allodynia induced by MMP-9 and SNL is reversed by IL-1 $\beta$  neutralizing antibody (5  $\mu$ g, i.t.,  $* p < 0.05, n = 6$ ). **(g)** Schematic representation of MMP-9-triggered sequential events for the genesis of neuropathic pain. MMP-9 upregulation after nerve injury increases IL-1 $\beta$  cleavage in the DRG and spinal cord. MMP-9 and IL-1 $\beta$  are transported to spinal central terminals. Dashed arrows indicate previously known events. A positive feedback loop between IL-1 $\beta$  and p38 can enhance the production of IL-1 $\beta$ , leading to increased pain sensitivity.

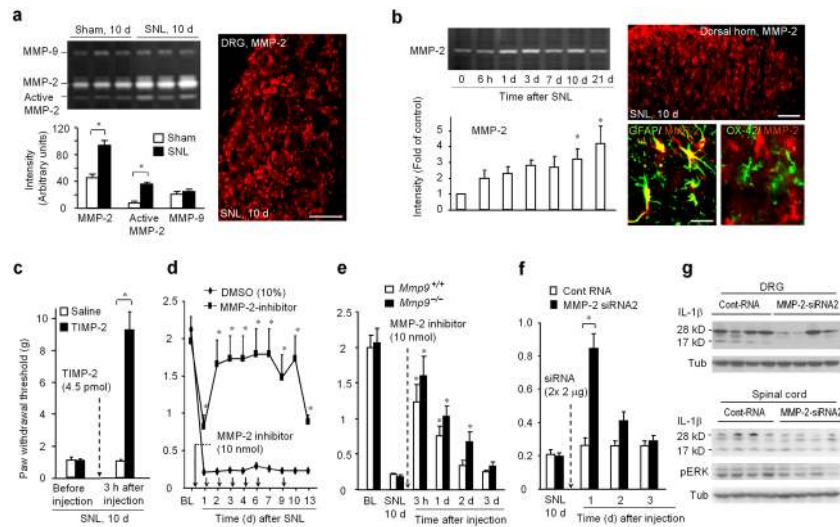


**Figure 4. MMP-2 upregulation after SNL maintains neuropathic pain via IL-1 $\beta$  signaling and ERK activation in spinal astrocytes**

(a) Gelatin zymography reveals MMP-2 upregulation in rat DRGs 10 days after SNL. Low panel, intensity of MMP bands ( $* p < 0.05$ ,  $n = 3$ ). Right panel, MMP-2 expression in DRG satellite cells. Scale, 50  $\mu\text{m}$ . (b) Gelatin zymography shows MMP-2 upregulation in rat dorsal horn after SNL. Lower panel, intensity of MMP-2 bands ( $* p < 0.05$ , compared to naive control,  $n = 5$ ). Upper right panel reveals MMP-2 expression in the ipsilateral superficial dorsal horn. Scale, 50  $\mu\text{m}$ . Lower right panel shows double staining of MMP-2 with GFAP and OX-42. Scale, 10  $\mu\text{m}$ . (c) Reversal of SNL-induced mechanical allodynia by TIMP-2 (4.5 pmol, i.t.) in SNL rats ( $* p < 0.05$ ,  $n = 6$ ). (d) Repeated daily injections of a synthetic MMP-2 inhibitor (10 nmol, i.t.) persistently attenuates SNL-induced allodynia in mice ( $* p < 0.05$ , compared to corresponding vehicle,  $n = 5$ ). (e) Reversal of SNL-induced allodynia by the MMP-2 inhibitor (10 nmol, i.t.) in both MMP-9 knockout and wild type mice. Note that MMP-2 inhibitor is more effective in knockout mice ( $* p < 0.05$ , compared to respective pre-injection baseline,  $n = 5$ ). (f) Reversal of SNL-induced mechanical allodynia by MMP-2 siRNA2 (2 $\times$ 2  $\mu\text{g}$ , i.t.) in mice ( $* P < 0.05$ ,  $n = 6$ ). (g) MMP-2 siRNA2 treatment (2  $\times$  2  $\mu\text{g}$ , i.t.) inhibits IL-1 $\beta$  cleavage in the DRG and dorsal horn (78% and 29% reduction of 17 kD band, respectively,  $p < 0.05$ ) and ERK activation (39% reduction of pERK1/2 bands,  $p < 0.05$ ) in the dorsal horn of SNL mice (day 10).